# Collapse Dynamics of Block Copolymers in Selective Solvents: Micelle Formation and the Effect of Chain Sequence

**I. R. Cooke* and D. R. M. Williams**

*Research School of Physical Sciences, Australian National University, Canberra, ACT 0200, Australia*

*Received May 14, 2002*

ABSTRACT: Using Langevin dynamics simulations, we examine the effect of chain sequence on the thermodynamics and kinetics of heteropolymer collapse. We employ a bead−spring model with two monomer types: one for which the solvent is good and the other, poor. Steady-state results indicate that the collapse of large block chains occurs over a wide temperature range. The collapsed state is well-defined in the case of small block chains and consists of a string of unimolecular micelles. We follow the kinetics of collapse by measuring the number of clusters $N_c$ and the radius of gyration $R_g$ over time, starting from an instant temperature quench. Our results are in agreement with the well-known model of collapse in which cluster formation occurs rapidly and is followed by cluster aggregation. The details of this cluster formation and coalescence mechanism differ strongly depending on block size, and this in turn is found to affect the overall rate of collapse.

## 1. Introduction

A single chain homopolymer in a good solvent assumes a diffuse coil state whereas in a poor solvent it forms a dense globule.[1] The collapse from a coil to a globule is a transition that has been relatively well described for a homopolymer. Although some further transitions have recently been described at low temperature,[2,3] the thermodynamics of the basic collapse are relatively well understood, from both theory[4,5] and numerical simulation.[6] The kinetics of homopolymer collapse are also now well understood and have been studied via a number of different theoretical approaches[7−10] as well as numerical simulations.[10−12]

A coil−globule transition also occurs for heteropolymers with a sufficient proportion of poor solvent monomer.[10] This case is of special interest as a model for the folding of biopolymers such as DNA and proteins. Elucidating the fundamental physics of heteropolymer collapse presents a considerable challenge compared with the simple homopolymer case. In particular, the composition and sequence of monomers in the backbone chain greatly increases the complexity of the problem. Biopolymers such as DNA and proteins represent an extreme example of this complexity. They have sequences which are "designed" by the process of evolution and which contain up to 20 different monomer types. Much recent research has attempted to design sequences with desired properties (e.g., rapid folding to a native state) in a manner that mimics biological evolution.[13,14] An interesting feature of these designed sequences is that they often display a well-defined structure in which similar monomers associate in blocks.[15] Inspired by this basic observation, our aim is to determine the fundamental effects of block size on the thermodynamics and kinetics of polymer folding. Obviously, such work applies not only to biopolymers but also to synthetic polymers which often polymerize in such a way as to form associations or blocks of identical monomers. Indeed, our work much more closely models synthetic polymers for we ignore bond stiffness in the system, which can play an important role in most biopolymers.

Given that the dominant driving force for polymer collapse is solvent−monomer interaction, the most obvious means of differentiating between monomers in a sequence is through their hydrophobicity, $\epsilon$. Copolymers where $\epsilon$ is assigned as a Gaussian random variable to each monomer have been studied through both simulation[16] and theory.[17] In the study of Timoshenko et al.,[17] it was shown that the kinetics of collapse for random heteropolymers involves at least two, sometimes three, distinct stages. The earliest of these stages is thought to involve the rapid formation of clusters along the chain, in a manner similar to homopolymer collapse. Following this stage, the clusters coalesce at a rate that depends on the dispersion $\Delta$ of $\epsilon$.[17] In polymers with particularly large dispersion a third kinetic stage involving rapid rearrangement to a more compact globule is predicted.

Another class of polymer sequences exists where $\epsilon$ is assigned as a binary variable 0 or 1. These sequences represent the simplest type of heteropolymers but retain the basic tendency for phase separation of monomer types. It is relatively simple to define different sequence structures for such polymers, and they are the natural choice for our investigation of block size. Previous work on the kinetics of collapse for binary polymers suggests that it proceeds in a superficially similar manner to that of homopolymers, i.e., an initial cluster formation phase followed by cluster coalescence.[16,18,19] Despite this similarity, we show later that the heteropolymer collapse exhibits some key differences from that of a homopolymer.

In this work we find that microphase separation plays an important role in both the thermodynamics and kinetics of collapse for heteropolymers with various block sizes. This point is emphasized throughout. As a matter of interest, it is also notable that this microphase separation often gives rise to compact states in the form of connected strings of intrachain micelles. The existence of strings of such micelles was predicted in the thermodynamic limit by Halperin[20] and has been observed in simulations and experiments on branched, comblike heteropolymers[21,22] and straight-chain heteropolymers.[19,23] Intramolecular polymeric micelles are believed to have promise as agents for drug delivery.[24]

10.1021/ma020741f CCC: $25.00 
Published on Web 02/27/2003

## 2. Details of Model and Simulations

**2.1. General.** Our heteropolymer model is of the bead−spring type.[25] In this model, the bead size provides a simple means of accounting for excluded-volume interactions while the springs provide chain connectivity and represent a statistical segment of identical monomers. The excluded-volume interaction is modeled as a repulsion of the form

$$V_{ev}(i,j) = 4\epsilon\left(\frac{\sigma}{r(i,j)}\right)^{12} \quad (1)$$

Here $\sigma$ is a constant that sets the length scale over which excluded-volume interactions are dominant, and $r(i,j)$ is the distance between beads $i$ and $j$. Adjacent beads in the chain also interact via an entropic spring potential

$$V_{sp}(i,i+1) = \frac{3k_BT}{2a^2}(\mathbf{r}_i - \mathbf{r}_{i+1})^2 \quad (2)$$

Here $\mathbf{r}_i$ is the position vector of the $i$th bead, $k_B$ is Boltzmann's constant, and $T$ is the temperature. The average value of the distance squared between adjacent beads, $\langle(\mathbf{r}_i - \mathbf{r}_{i+1})^2\rangle$ is represented by $a^2$.

Two types of beads are used, hydrophobic H and polar P. The polymer is assumed to be in aqueous solvent so that HP and PP interactions are purely repulsive, while HH interactions are attractive. This attractive force is modeled by $V_{attr}(i,j)$ and is given by

$$V_{attr}(i,j) = -4\epsilon\left(\frac{\sigma}{r(i,j)}\right)^{6} \quad (3)$$

The constant $\epsilon$ determines the strength of HH attractions. The combination of eqs 1 and 3 results in a potential well located at $\sim\sigma$ with a depth of $\epsilon$, i.e., a Lennard-Jones potential.

Both steady-state and kinetic results in this work were obtained from solutions of the Langevin equation, which may be written in finite difference form as[25]

$$r_{\alpha_i}(t+\Delta t) = r_{\alpha_i}(t) - \frac{1}{\zeta}\frac{\partial V_i}{\partial \alpha_i}\Delta t + \eta(t)\sqrt{D} \quad (4)$$

Here $r_{\alpha_i}$ is a Cartesian component of the position vector $\mathbf{r}_i$ (i.e., $\alpha = x, y, z$). The potential $V_i$ is the total potential for bead $i$, obtained as a combination of eqs 1−3. $D$ is the diffusion constant, $D = k_BT/\zeta$, $\Delta t$ is the simulation time step, and $\zeta$ is a quantity called the friction. $\zeta$ is related to the solution viscosity $\eta_s$ and the radius of the hydrodynamic particles $h$ according to the relation $\zeta = 6\pi\eta_s h$ (note that $h \sim \sigma/2$). The random fluctuations caused by the motion of solvent particles are accounted for through the term $\eta(t)\sqrt{(D)}$, where $\eta(t)$ is a stochastic variable that is given by a Gaussian distribution with mean 0 and variance $2\Delta t$. It should be remembered that hydrodynamic interactions between monomers are neglected in this model the system is assumed to be free-draining.

Throughout this work we will make use of dimensionless variables which we define as follows. Denoting dimensionless quantities with an asterisk, we have $T^* = 2k_BT/\epsilon$ and $t^* = (2/0.7^2)t\epsilon/\zeta\sigma^2$, where $T$ is the temperature and $t$ is time. Later, we encounter the radius of gyration $R_g$ and the internal energy $U$, which have reduced quantities defined by $R_g^* = 0.7R_g/\sigma$ and $U^* = 2U/\epsilon$. We choose the numerical values of $\epsilon = 2$, $\zeta = 1$, and $\sigma = 0.7$ such that all dimensionless quantities have the same numerical value as the corresponding real quantity. Because of the numerical equality between dimensionless and real quantities, we refer to dimensionless quantities without the asterisk. The units of the corresponding real quantity can be found from the relationships mentioned above.

To speed up calculation of $\partial V_i/\partial x_i$ at each time step, the potentials $V_{attr}$ and $V_{rep}$ were cut off at $r(i,j) = 2.5\sigma$, and a Verlet nesting list was used to keep track of near neighbors. We found it necessary to use a relatively small time step, $\Delta t = 0.0001$.

All simulations were initialized by taking a random walk as the starting configuration and equilibrating at the starting temperature for $2 \times 10^7$ time steps. Ensemble averaging was performed by making 50 individual simulation runs from different starting configurations.

**2.2. Chain Sequence Construction.** Since our aim was purely to study the effect of block size, we conducted all simulations with a fixed overall chain length of $N = 180$ monomers and fixed H:P ratio of 1:1. We examined families of polymer chains with sequence types that were either regular or probabilistic. The regular chain sequences were of the form $(90/n)(n\mathrm{H}n\mathrm{P})$, where $n$ is the size of contiguous H or P blocks. Probabilistic sequences were defined according to the tendency for H or P type monomers to associate in blocks. This tendency is expressed by the probability $\phi$ that a monomer of a given type will polymerize adjacent to a monomer of the same type. Larger values of $\phi$ result in larger block sizes, such that $\phi = 0.5$ generates random sequences, $\phi < 0.5$ represents sequences with a tendency toward alternating bead type, and $\phi > 0.5$ gives rise to sequences with large blocks. Under this definition, $\phi$ is closely linked to the chemical process of polymer synthesis; however, it is also incompatible with the constraints of fixed H:P ratio and fixed chain length. This problem becomes apparent when one considers the sequence production process, in which beads are added one at a time according to the probability $\phi$. Toward the end of this process, the number of H or P type beads inevitably reaches its maximum value (in this case 90), and the remaining beads are then automatically assigned the opposite type, so as to maintain an H:P ratio of 1:1. The obvious consequence of this is that the size of end blocks will be slightly larger than blocks in the rest of the chain. In principle, one might expect that these end blocks could modify the collapse kinetics. This possibility is discussed in the context of our kinetics results, presented in section 4.

## 3. Steady-State Properties

We studied the steady-state properties of HP chain sequences as a function of temperature. To obtain steady-state conditions, the chains were cooled at successively slower rates from $T = 4$ to $T = 0.1$ until further slowing did not result in any change in the appearance of plots of observable vs $T$.

The main qualitative results are shown in Figure 1. It is clear that we get a series of micelles along the chain. Such multiple micelle states have been observed previously using Monte Carlo simulations[10] and as metastable states in free energy minimization studies.[19,23]

As indicators of the state of polymer collapse, we tracked two observables, the radius of gyration $R_g$ and

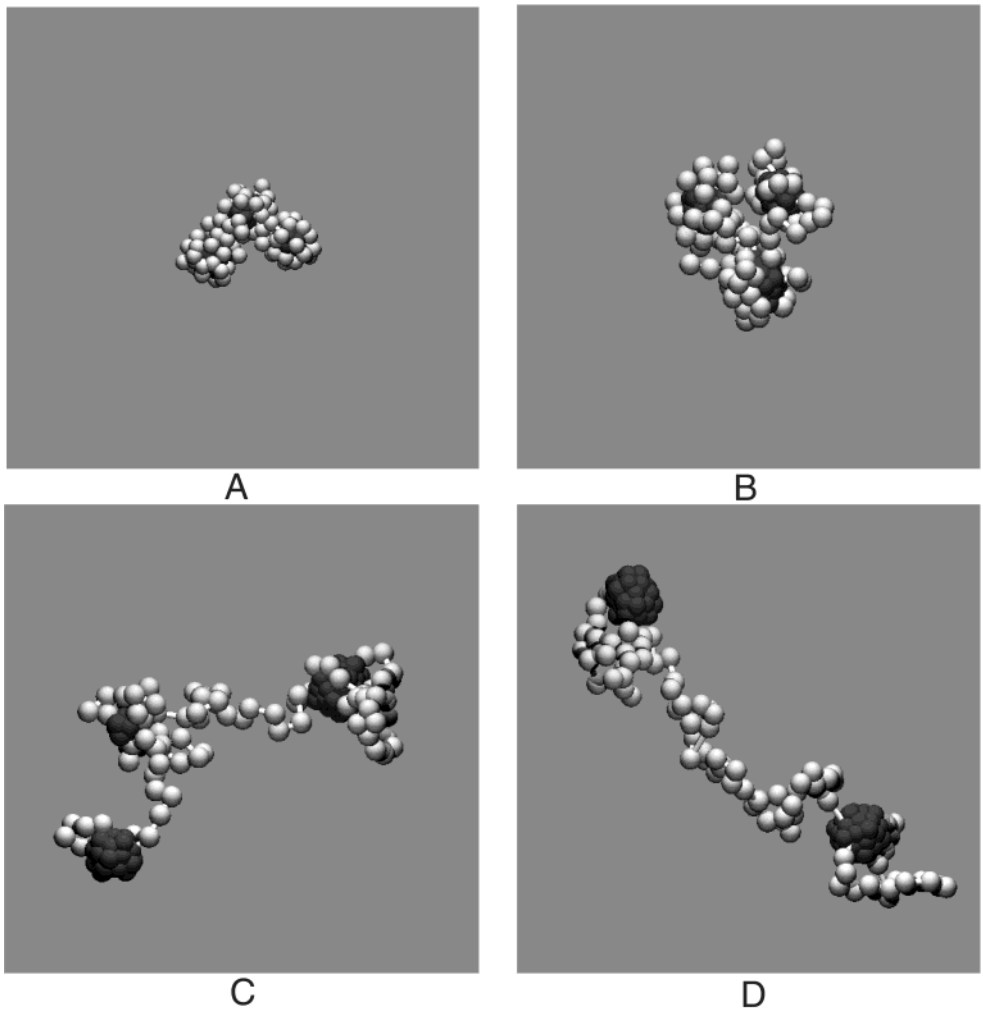


**Figure 1.** Snapshots of the final collapsed state for polymers with chain sequences corresponding to $\phi = 0$ or $n = 1$ (A), $\phi = 0.5$ (B), $\phi = 0.9$ (C), and $\phi = 0.98$ (D).

internal energy $U$, which are given by eqs 5 and 6, respectively.

$$R_g^2 = \frac{1}{N}\sum_i^N (\mathbf{R}_{cm} - \mathbf{r}_i)^2 \tag{5}$$

$$U = \frac{1}{N}\sum_{ij}(V_{ev}(i,j) + C(i,j)V_{attr}(i,j)) \tag{6}$$

Here $\mathbf{R}_{cm}$ is the center of mass of the polymer, and the function $C(i,j)$ takes a value of 1 when $i$ and $j$ are both H type monomers and 0 otherwise. Note that the internal energy does not include the spring energy $V_{sp}$, which is of a purely entropic origin. Although it is clear that collapse from a coil to a globule should be detectable as a decrease in either $R_g$ or $U$, we have found that $U$ is also sensitive to more subtle changes in the polymer structure. To avoid repetition, we focus primarily on measurements of $U$ and present results for $R_g$ only where they differ qualitatively from those of $U$.

Both regular block size and probabilistic chains show a strong decrease in $U$ as $T$ is lowered from 4 to 0.5 (Figure 2). Since this decrease is accompanied by a corresponding change in the radius of gyration $R_g$ (Figure 4), it is interpreted as a collapse transition. The collapse becomes more gradual ($\Delta T_{collapse}$ increases) as the chain sequence block size is increased.

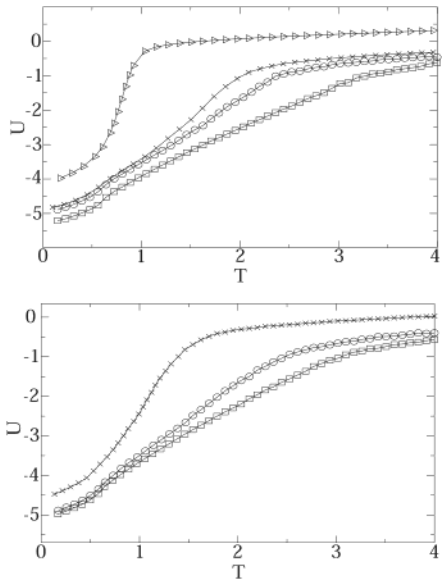


**Figure 2.** Internal energy per monomer, $U$ vs $T$, for regular block (top plot) and probabilistic (lower plot) type chains. In the top figure the chain types are $n = 1$ (▽), $n = 10$ (×), $n = 18$ (○), and $n = 90$ (□). In the lower figure the chain types are $\phi = 0.5$ (×), $\phi = 0.9$ (○), and $\phi = 0.98$ (□).

Superimposed on the large scale collapse transition, it is possible to observe a small but sudden decrease in

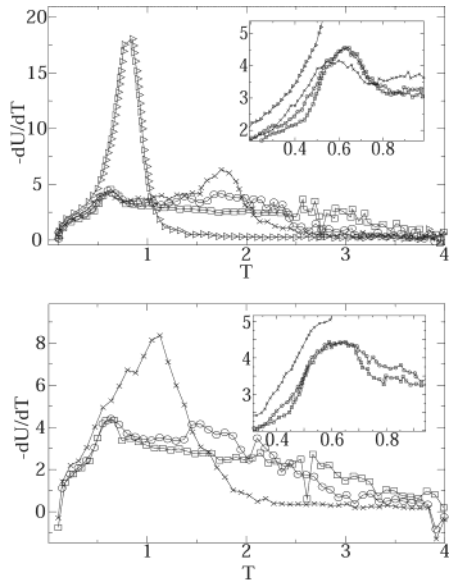


**Figure 3.** Plots of the quantity $-\mathrm{d}U/\mathrm{d}T$ vs $T$ for regular block (top plot) and probabilistic (lower plot) type chains. Chain types and corresponding symbols are identical to those of Figure 2. In the top figure, $n = 1$ (▽), $n = 10$ (×), $n = 18$ (○), and $n = 90$ (□). In the lower figure, $\phi = 0.5$ (×), $\phi = 0.9$ (○), and $\phi = 0.98$ (□). An inset in each plot shows details of the region surrounding the "freezing" peak mentioned in the text.

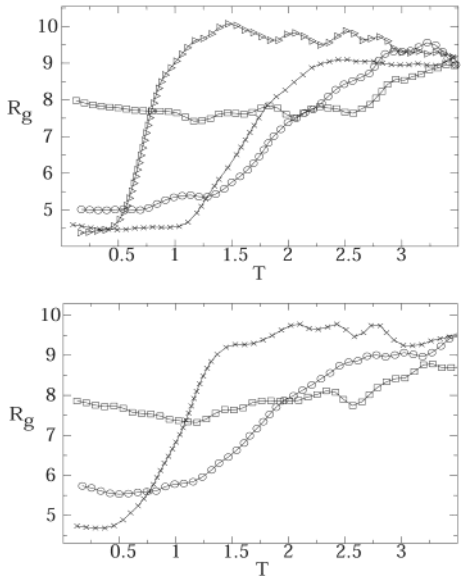


**Figure 4.** Radius of gyration $R_g$ vs $T$ for regular block (top plot) and probabilistic (lower plot) type chains. Chain types and corresponding symbols are identical to those of Figure 2. In the top figure, $n = 1$ (▽), $n = 10$ (×), $n = 18$ (○), and $n = 90$ (□). In the lower figure, $\phi = 0.5$ (×), $\phi = 0.9$ (○), and $\phi = 0.98$ (□).

$U$ at $T \sim 0.6$. This low-temperature decrease in $U$ is more clearly evident as a small sharp peak in plots of $-\mathrm{d}U/\mathrm{d}T$ vs $T$ (Figure 3). Although this low-temperature peak is small, it appears to be universal since it occurs for all chain sequence types except those with very small block size, where it is replaced by a low-temperature collapse peak. Our view is that this low-temperature peak might correspond to a globule-to-globule transition such as, for example, from fluidlike to solidlike phases. Since this work is primarily concerned with the coil-to-globule transition, we did not study this second transition in detail, and we cannot be sure of its precise nature. It is convenient to refer to this low-temperature transition as "freezing" although in using that term we do not necessarily claim that it involves a fluid-to-solid transition. Although our study of the "freezing" transition is far from complete, we present our observations here in the context of recent homopolymer studies where similar transitions have been observed. For example, multiple distinct peaks in the heat capacity have been observed for beads attracted by square well potentials,[2,3] and more recently, a similar result was observed for Lennard-Jones homopolymers.[26,27] In the square well study three distinct peaks were observed in the heat capacity. On the basis of bead fluctuations, these were interpreted as being analogous to gas−liquid, liquid−solid, and solid−solid transitions. Experimental evidence also exists[28] to indicate that initial polymer collapse leads to a molten globule, which can then undergo a further transition to a solid as $T$ is lowered. As a final point, it is worth noting that the indistinct nature of the low-temperature peaks in our study is probably due to finite size effects and for real polymers the "freezing" transition should be much more prominent.

Although the internal energy $U$ is the parameter that is most sensitive to structural changes, it is also possible to observe the collapse transition as a change in the radius of gyration $R_g$ (Figure 4). The change in $R_g$ across the collapse transition is most dramatic for small block size, since in this case, chain connectivity requires that the collapse of H type beads must be accompanied by a corresponding collapse of the P. This is illustrated by Figure 1, which shows the collapsed configurations for polymers with $\phi = 0$, 0.5, 0.9, and 0.98 (regular block chains are similar in appearance). In the cases where $\phi = 0$ and $\phi = 0.5$ the collapsed state consists of clusters of H type beads surrounded by short loops of P, in structures that resemble intrachain micelles. This contrasts with the case of large blocks, for which the H regions collapse independent of the P, leaving the P type monomers to form long diffuse loops between the H regions. These diffuse loops allow $R_g$ to remain large.

We now turn our attention to the final compact state formed for chains with small block size. This state resembles a chain of micelles (Figure 1), where each micelle consists of a dense core of H type beads surrounded by P. Since our simulations calculate internal energy rather than free energy, it is difficult to assess whether this chain of micelles represents a global free energy minimum or a kinetically trapped, local minimum. Plausible theories exist for either of these scenarios. At the extreme of large block size and chain length, Halperin[20] provides scaling arguments based on deformation of P type loops, which predict a chain of micelles as the free energy minimum. In our simulations we cannot expect Halperin's arguments to hold because the block size is never large enough to form a true brush. More relevant to this study is the case of small block size for which it is also possible to see why a chain of micelles might be favored over a single large one. Consider, for example, an alternating HP copolymer in which the globule core radius $r$ is larger than the equilibrium HP bond length $a$. In that case, an H type bead at the center of the core must stretch to connect with its corresponding P bead outside the core, or else the P bead must become incorporated into the core. Both options involve a strong free energy penalty. This suggests that the upper limit for micelle size occurs

when $r \sim a$. If $f$ is the number of blocks per micelle and $r_b$ is the bead radius, then $a \sim f^{1/3} r_b$. Since the average number of micelles per chain $m$ is given by $m = N/(2nf)$, we have $m \sim N r_b^3/(2na^3)$. For the parameters used in our simulation this should give $m \sim 3$ for $n = 1$ and $m \sim 1$ for $n > 1$, which suggests that chain connectivity could be driving the micelle separation in the alternating $n = 1$ case but that it is probably not important for larger $n$.

The alternative possibility, that the multiple micelle state is a kinetically trapped state, is consistent with the collapse kinetics of heteropolymers. As we verify in a later section, the heteropolymer chain collapses via the initial formation of small globules which gradually coalesce. In such a regime it is not difficult to envisage a point at which the micellar coronas of globules become sufficiently large that they effectively shield the attractive forces between the cores of H type beads. In principle, this shielding could result in a kinetically stabilized chain of micelles. Similar metastable states have been observed using the GSC method[19] and also by direct free energy minimization.[23,29] In all these studies the number of monomers was relatively small ($N < 60$) as in the present work, and it was found that the multiple micelle state represents a local free energy minimum with the global minimum being a single phase separated globule. With the possible exception of the alternating HP chain (see above), it therefore seems likely that this is also true of the multiple micelle states observed in our study.

## 4. Kinetics

In this section we investigate the dynamics of collapse following an instantaneous quench from high temperature $T^+$ to low temperature $T^-$. $T^+$ is chosen to be well above transition temperature, and $T^-$ is chosen to be well below but not so low as to result in impracticably slow dynamics. All simulations involved an initial equilibration period of $2 \times 10^7$ time steps at $T^+ = 20$ followed by an instantaneous quench to $T^- = 0.3$. We measured time from the moment of the quench, and at successive time steps the state of the polymer chain was characterized by various observables, including the internal energy $U$, the radius of gyration $R_g$, and the number of clusters $N_c$ and by visualization. $N_c$ was calculated by defining a cluster radius $r_c = 3\sigma/2$ such that two beads whose separation is less than $r_c$ are defined as belonging to the same cluster. A cluster only counted toward $N_c$ if it contained more than a single bead. In addition, only H type beads that were not adjacent along the chain were used to define a cluster. The algorithm used for computation of $N_c$ is described in detail by Sevick et al.[30]

**4.1. Cluster Formation and Coalescence.** In Figure 5 we plot $N_c$ against $\ln(t)$ for regular block and probabilistic chains. The main feature of all the curves in these plots is a single peak in $N_c$, the presence of which is consistent with a two-phase collapse process involving cluster formation followed by cluster coalescence. This mechanism is also evident in Figure 6, which shows snapshots of three different chain types at various stages of collapse. For each of the chain types the initial state is that of a random coil. At the location of the peak in $N_c$ this coil has collapsed into a number of smaller clusters, and at still later times these clusters have coalesced.

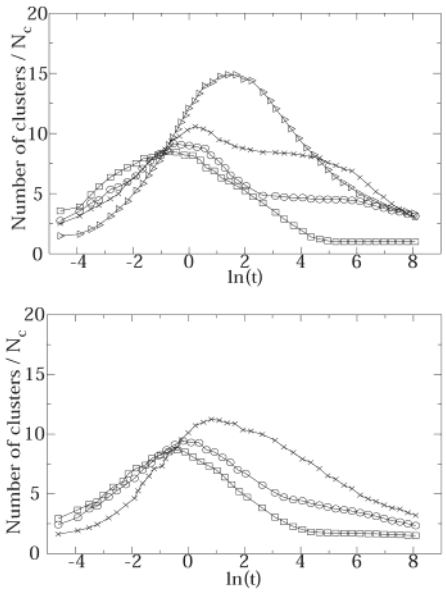


**Figure 5.** Number of clusters $N_c$ vs $\ln(t)$ for both regular block (top plot) and probabilistic (lower plot) type chains. In the top figure, the chain types are $n = 1$ (▽), $n = 10$ (×), $n = 18$ (○), and $n = 90$ (□). In the lower figure, the chain types are $\phi = 0.5$ (×), $\phi = 0.9$ (○), and $\phi = 0.98$ (□).

Although all backbone chain types seem to follow a basic cluster formation and coalescence mechanism, there is substantial variability within this basic framework. For example, chains with small blocks exhibit a much greater maximum number of clusters, $N_c^{max}$, than those with larger blocks, and this $N_c^{max}$ occurs at a much later time. Examination of snapshots of different polymer chains during collapse indicates several structural differences. Although we speculate on the manner in which these structural differences affect the kinetics, it is beyond the scope of this work to establish which of the possible mechanisms is dominant. Initially, we consider chains at the extremes of small and large block size $n = 1$ and $n = 90$. In the $n = 1$ case the clusters resemble miniature micelles with a core of H and a corona of P (Figure 6), whereas in the large block chain the clusters are comprised purely of H type monomers. In principle, these two cluster types should differ in both their mode of formation and mode of coalescence. The formation of clusters in the $n = 90$ case involves clustering of like monomers within a single block of H; however, for the $n = 1$ chain, the micelle-like clusters can only form via the union of blocks which were initially separate along the chain. Coalescence of these micelle-like clusters is clearly different from that of pure H clusters due to the presence of a shielding corona of P type monomers.

So far we have only looked at two extremes of block size. Between these extremes, the behavior of $N_c$ vs $\ln(t)$ exhibits some further features of interest. In particular, it is here that we see some differences between the regular block type chains and the probabilistic chains. For regular block type chains with $n = 18$ and $n = 10$ there is an initial rapid increase in $N_c$ followed by a slight decrease and then a plateau which terminates in a final sharp decrease. In both cases the value of $N_c$ in the plateau region is close to the total number of H type blocks in the original chain, i.e., 9 for $n = 10$ and 5 for $n = 18$. This fact, combined with snapshots of the $n = 10$ polymer shown in Figure 6, leads us to the following picture for the collapse of intermediate block

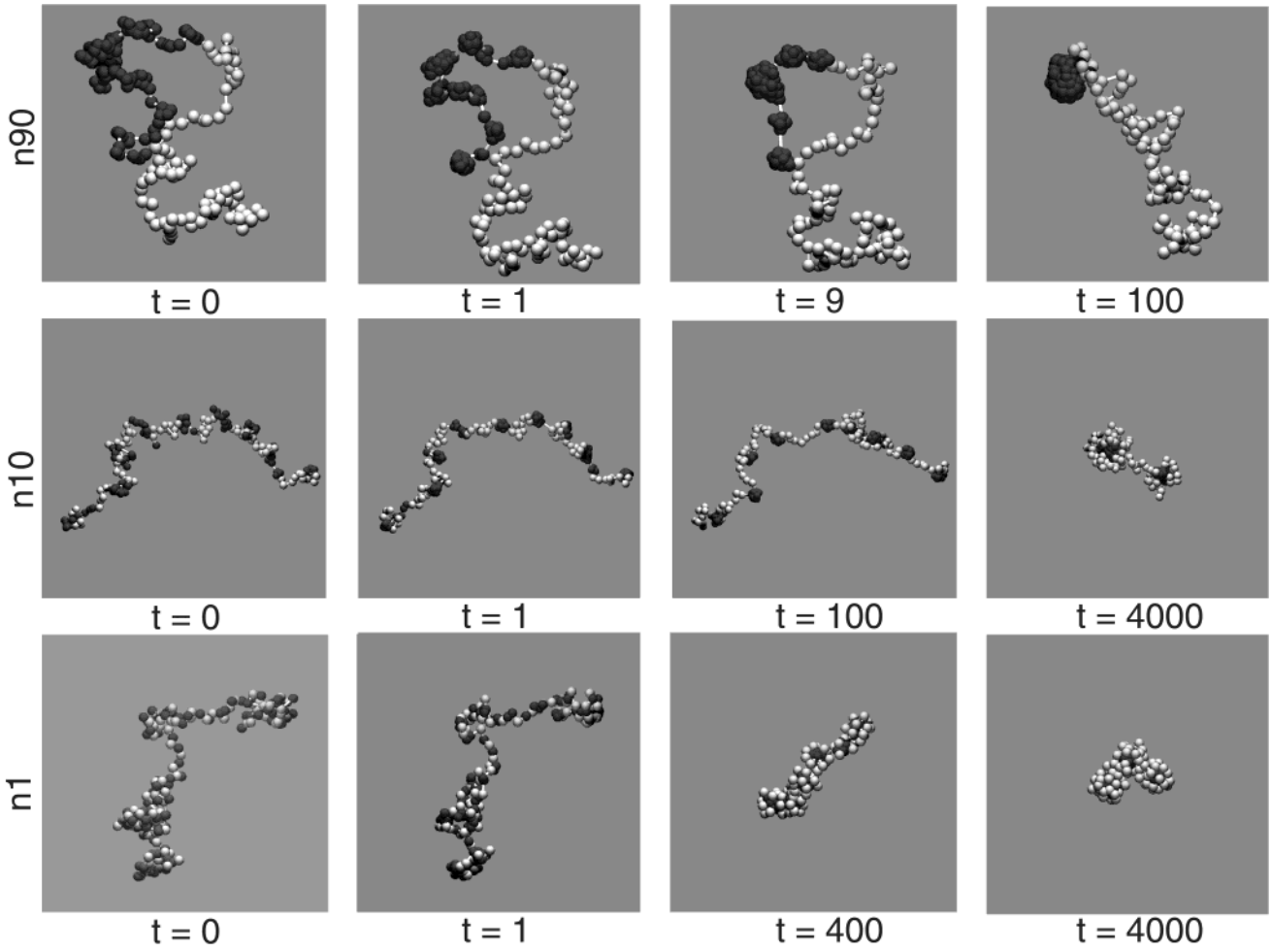


**Figure 6.** Snapshots of three different polymer chain types at representative stages of collapse.

size type chains. Initially, collapse occurs within blocks with some blocks producing more than one cluster. After a short time, all intrablock clusters have coalesced, leaving a number of clusters roughly equal to the number of blocks. As a consequence of the regular block sequence, each cluster of H monomers should be separated along the chain by an equal length of P. Since solvent-mediated attractions between the H type clusters are relatively short range, it is necessary for the clusters of H to diffuse within a certain capture radius $b$ before they coalesce to a larger cluster. Below, we provide a rough estimate of the time scale for this diffusion and shall see that it is consistent with the length of plateau regions in Figure 5. In making this estimate, we assume that the H clusters are not shielded by the P and are free to diffuse within the volume occupied by the polymer. Snapshots of an intermediate block size polymer indicate that the conformation immediately after the initial intrablock collapse is made up of relatively unshielded clusters of H. After a certain number of these clusters have coalesced, it is clear that a shielding corona of P should form. In our estimate below we assume that the unshielded state persists at least until the original cluster number is reduced to half. This seems reasonable since it means that, on average, each original cluster has coalesced with just one other cluster.

To calculate the rate of cluster coalescence in a polymer of intermediate and regular block size, we assume that the process is analogous to a diffusion-controlled chemical reaction, for which the appropriate dynamical equation is[31]

$$\frac{\mathrm{d}\rho(t')}{\mathrm{d}t} = -8\pi\rho(t')^2 Db \tag{7}$$

where the reaction involves only one reactant, in this case clusters of H type monomer. The number density of these clusters is $\rho(t')$, and their diffusion coefficient is $D$. $t'$ represents time that is measured from the point at which clusters form but have not yet coalesced. This definition for $t'$ is quite ambiguous; however, the time scale for diffusion is so long compared with the time required for initial cluster formation that there is negligible difference between $t'$ and $t$. The capture radius $b$ represents the distance from the center of a cluster, within which coalescence becomes highly likely. A logical choice for $b$ in our case is the Lennard-Jones cutoff distance $2.5\sigma$ plus the cluster radius $n^{1/3}\sigma/2$. Since the clusters are part of a polymer chain, they are initially confined to a volume that is a function of the overall radius of gyration for the entire chain $R_g$. Assuming that each block forms a single cluster at time $t' = 0$, the initial value of $\rho$ is

$$\rho(0) = \frac{m_0}{\frac{4}{3}\pi {R_{g0}}^3} \tag{8}$$

where $m_0$ is the number of clusters at $t' = 0$ and is given

by $m_0 = N/2n$, and $R_{g0}$ is the radius of gyration at $t' = 0$. Solving eq 7 for $\rho(t')$ with this initial condition, we obtain eq 9.

$$\rho(t') = \frac{1}{8bD\pi t' - \frac{4\pi {R_{g0}}^3}{3m_0}} \tag{9}$$

Now we assign the characteristic time $t'_c$ to the time required for half the clusters to disappear on average. Solving for $t'_c$, we obtain

$$t'_c = \frac{{R_{g0}}^3}{2bDm_0} \sim \frac{\sigma^3 N^{4/5} n^{2/3} \zeta}{k_B T} \tag{10}$$

Now since $t'_c$ is roughly proportional to $n^{2/3}$, we expect that larger block sizes should give longer diffusion times. The plateau regions in Figure 5 for $n = 10$ and $n = 18$ follow this pattern.

Probabilistic chains with intermediate block size exhibit $N_c$ vs $\ln(t)$ curves that contain much less obvious plateau type features than those of fixed block chains. As an example, we consider the $\phi = 0.9$ type chain which has a mean block size of ~10 and in that sense is equivalent to an $n = 10$ regular block chain. Although the $\phi = 0.9$ chain does show a distinct decrease in the slope of $N_c$ vs $\ln(t)$ at $\ln(t) \sim 3.5$, this is not nearly as pronounced as the plateau exhibited by the $n = 10$ chain. Our reasoning for this is that the range of block sizes present in probabilistic chains acts to smooth the $N_c$ vs $\ln(t)$ curves. In this sense one envisages some clusters separated by relatively short lengths of P type monomers and some separated by larger sections of P. Since the average coalescence time depends on the size of the intervening P block, this situation should produce a range of coalescence times and hence a smoothed $N_c$ vs $\ln(t)$ curve. It is also possible that the presence of a range of block sizes could speed up the overall rate of coalescence. This could occur simply because early coalescence of some clusters leads to a decrease in the system volume and hence an increased capture rate for the remaining clusters.

**4.2. Kinetics of the Radius of Gyration.** In Figure 7 we present plots of $R_g$ against $t$ for fixed block and probabilistic chains. First, it is quite clear that the block size has a strong effect on the final value of $R_g$ to which the chain collapses. This makes it difficult to compare absolute rates of collapse; however, the general trend is fairly clear. For the very large blocks ($n = 90$, $\phi = 0.98$) the collapse is rapid, occurring completely by $t < 100$. The collapse of very small blocks ($n = 1$, $\phi = 0.5$) is not as rapid as for large blocks, but it does appear to be complete by the end of the simulation $t < 4000$. In contrast, the intermediate block size chains undergo extremely gradual collapse that is clearly not complete by the end of the simulation $t > 4000$. Thus, we can summarize the effect of block size on collapse rate by saying that very large blocks are fastest, very small blocks are the next fastest, and intermediate blocks are slowest. These rates of collapse reflect the distinct collapse mechanisms for large, small, and intermediate blocks. Also of interest in this regard are the general shapes of the collapse curves, which for intermediate block size chains are close to linear while for small and large block size they resemble exponential decay.

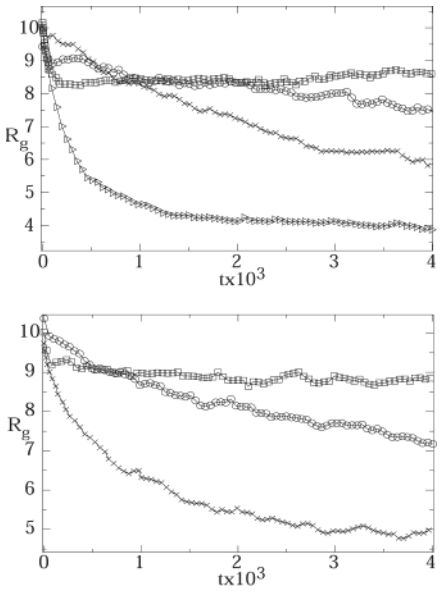


**Figure 7.** Radius of gyration $R_g$ vs time $t$. Both regular block (top plot) and probabilistic (lower plot) type chains are shown. Chain types and corresponding symbols are identical to those of Figure 5. In the top figure, $n = 1$ (▽), $n = 10$ (×), $n = 18$ (○), and $n = 90$ (□). In the lower figure, $\phi = 0.5$ (×), $\phi = 0.9$ (○), and $\phi = 0.98$ (□).

The patterns noted above may be interpreted in the context of the pictures of collapse shown in Figure 6. In the case of very large block size polymers the collapse is entirely homopolymer-like and occurs freely without the interference of P type monomers. Not surprisingly, this results in relatively rapid collapse. At the opposite extreme of block size, the very small block chains can only collapse through the joining of monomers that were initially separate along the chain sequence. This joining results in the formation of clusters, which in turn coalesce. Since these clusters are surrounded by a corona of P, they must overcome a free energy barrier to coalescence. As the clusters coalesce, we expect that the energy barrier should increase (due to thickening of the corona) until eventually the collapse is complete or the system is trapped in a metastable state. This picture is consistent with the general shape of the $R_g$ vs $t$ curve for small block size in Figure 7, which displays rapid initial collapse that gradually slows and eventually stops.

For intermediate block size chains the situation is quite different. Snapshots of the polymer in Figure 6 as well as our arguments of section 3 suggest that this difference stems from the fact that H blocks are separated by distances larger than the Lennard-Jones cutoff, and therefore the collapse for intermediate block size polymers is largely dependent on the diffusion time for clusters. This diffusion-mediated collapse seems to result in an $R_g$ vs $t$ plot that is roughly linear over the time scales of our study.

A qualitatively similar comparison of collapse rates for different block size polymers has been performed using the GSC method on a polymer of length $N = 60$.[19] In that work the general shapes of the $R_g$ vs $t$ curves were similar to those of Figure 7. In particular, the $n = 3$ chain in that work displayed close to linear behavior for $R_g$ vs $t$, whereas the $n = 1$ and homopolymer chains both decayed much more rapidly.

Having given consideration to the mechanisms of collapse for different block sizes, it should be clear that

**Table 1. Fitting Results for the Relation $R_g^2 = A - Bt^Q$ Fitted to the Data of Figure 7, Where $R_g$ Is the Radius of Gyration, $t$ Is Time, $A$ and $B$ Are Free Variables, and $Q$ Is the Exponent of Interest[a]**

Regular Chains

| $n$ | $Q$ | $\Delta Q$ |
|---|---|---|
| 1 | 0.60 | 0.03 |
| 10 | 0.62 | 0.03 |
| 18 | 0.61 | 0.02 |
| 90 | 0.86 | 0.09 |

Probabilistic Chains

| $\phi$ | $Q$ | $\Delta Q$ |
|---|---|---|
| 0.5 | 0.72 | 0.05 |
| 0.9 | 0.98 | 0.03 |
| 0.98 | 0.69 | 0.03 |

[a]The root-mean-square fitting error is given as $\Delta Q$.

these depend on system parameters such as the absolute block size and the strength and range of H−H attractions. With this in mind it is important to note that our main results are the mechanisms and rate-limiting factors rather than the absolute rates of collapse.

In mapping these results on to real polymers, it is important to consider exactly what is meant by intermediate, small, and large block size. Given that diffusion plays little or no role in the collapse of small block size chains, we should be able to define small in terms of the length scale over which hydrophobic interactions are important. Under this definition "small" should be such that the separation between blocks is less than the Lennard-Jones cutoff, i.e., $n^{3/5} < 2.5\sigma$. In our description of large block size collapse (above) all of the collapse occurred within blocks such that interblock coalescence is not important. On the basis of this idea, we define large block size polymers as those for which $n \sim N$. Intermediate block size polymers should lie somewhere between small and large, i.e., $2.5\sigma < n^{3/5}$ and $n < N$. If our results are to be applied to real polymers, then we see that it is important to know the value of $\sigma$ and also to assess the block size with respect to the overall chain length.

At early times after the quench we fit the kinetics results for each chain type to the power law $R_g^2 = R_{g0}^2 - At^Q$, where $A$ is an unknown constant and $R_{g0}$ is the radius of gyration at $t = 0$. Previous theoretical and simulation work[10,17,32] predicts that the exponent $Q$ should take the value 7/11 during the initial cluster formation stage of collapse. The end point of the initial cluster formation phase was taken as the location of the peak in $N_c$ (Figure 5), and the fitted exponents are given in Table 1. Agreement with the predicted exponenent of 7/11 was observed for large and intermediate block size fixed block chains but not for the alternating HP chain. Probabilistic sequences also show strong deviations from the value of 7/11 for $Q$, even in the case of relatively large blocks ($\phi = 90$). Despite these deviations, the general agreement is remarkably good, considering that the exponent 7/11 was originally derived only for a homopolymer.

At this point it should be emphasized that the results presented here do not include hydrodynamic interactions and assume the free draining or Rouse model. Hydrodynamics has been included in a small number of studies of the homopolymer collapse, either via the inclusion of explicit solvent[33,34] or using approximate theoretical approaches.[18] Pure hydrodynamics has been included for homopolymer collapse using the GSC method[18] and results in collapse mechanisms (i.e., cluster formation and coalescence) qualitatively similar to those observed in the absence of hydrodynamics. Although explicit solvent simulations account for hydrodynamics, it is important to recognize that they also introduce many-body interactions that become important as the monomer density increases (i.e., as collapse progresses). Explicit solvent studies so far seem to indicate a qualitatively different mechanism for the homopolymer collapse that is closer to uniform thickening along the chain than cluster formation and coalescence.[33,34] This suggests that explicit solvent effects, especially the many-body interactions, can be important in determining the mechanism of collapse for homopolymers. We note, however, that in our case uniform thickening along the chain is extremely unlikely due to the presence of P type monomers that break the chain up into separate blocks. For very small blocks, this breakup of the chain is not as pronounced, and it would be of some interest to conduct an explicit solvent simulation of collapse for the $n = 1$ case, which might show qualitatively different behavior.

As was pointed out in a previous section, the chain sequence production process for probabilistic chains results in a slightly larger block at the chain end. In considering how this end block might affect the collapse kinetics, we first note the qualitative similarity between results for probabilistic and regular block chains (for which there are no large end blocks). This similarity suggests that end block effects are minimal. The only point of difference in kinetics between regular and probabilistic chain types occurs for intermediate block size where the probabilistic chains exhibit a less pronounced plateau region. In a previous section, we provide some brief arguments for why this lack of a plateau could simply arise as a consequence of the inherent probabilistic nature of the chain sequence. Our view is that these arguments should still be valid and that end effects should be minimal, since the collapse in this case is largely determined by the diffusion-limited coalescence of H type clusters. In this regime the presence of intervening P blocks ensures that coalescence rates of all clusters are essentially independent.

## 5. Conclusions

The main qualitative feature of this study has been the ability to track and form a chain of micelles. We observed small micelle-like clusters as intermediates during collapse and larger micelle structures as part of the final collapsed state. We have established that monomer sequence can have a strong effect on the kinetics and thermodynamics of polymer collapse as well as the nature of the collapsed state.

We found a number of interesting features in the kinetics of collapse for heteropolymers of various block sizes. Regardless of the details of chain sequence, it was found that the basic kinetics of collapse could be described as rapid initial formation of clusters followed by cluster aggregation or coalescence. This observation is consistent with previous studies on homopolymers and random copolymers. We also observed considerable variation on this basic theme. The nature of the clusters differed considerably depending on block size, and this in turn was thought to influence the relative rates of cluster formation and coalescence. We found that chains could be classified into "small", "intermediate", and

"large" block sizes and that each of these classes is characterized by a distinct collapse mechanism.

## References and Notes


(1) Williams, C.; Brochard, F.; Frisch, H. L. *Annu. Rev. Phys. Chem.* **1981**, *32*, 433−451.
(2) Zhou, Y.; Karplus, M.; Wichert, J. M.; Hall, C. K. *J. Chem. Phys.* **1997**, *107*, 10691−10708.
(3) Zhou, Y.; Hall, C. K.; Karplus, M. J. *Phys. Rev. Lett.* **1996**, *77*, 2822−2825.
(4) Lifshitz, I. M.; Grosberg, A. Y.; Khokhlov, A. R. *Rev. Mod. Phys.* **1978**, *50*, 683−713.
(5) de Gennes, P. G. *J. Phys., Lett.* **1975**, *36*, L55−L57.
(6) Grassberger, P. *Phys. Rev. E* **1997**, *56*, 3682−3692.
(7) Buguin, A.; Brochard-Wyart, F.; de Gennes, Pierre, G. *C. R. Acad. Sci. Paris* **1996**, *322*, 741−746.
(8) Klushin, L. I. *J. Chem. Phys.* **1998**, *108*, 7917−7920.
(9) Halperin, A.; Goldbart, P. M. *Phys. Rev. E* **2000**, *61*, 565−573.
(10) Kuznetsov, Yu, A.; Timoshenko, E. G.; Dawson, K. A. *J. Chem. Phys.* **1995**, *103*, 4807−4818.
(11) Ostrovsky, B.; Bar-Yam, Y. *Europhys. Lett.* **1994**, *25*, 409−414.
(12) Sevick, E. M.; Williams, D. R. M. *Phys. Rev. Lett.* **1999**, *82*, 2701−2704.
(13) Shakhnovich, E. I.; Gutin, A. M. *Proc. Natl. Acad. Sci. U.S.A.* **1993**, *99*, 7195−7199.
(14) Yue, K.; Dill, K. A. *Proc. Natl. Acad. Sci. U.S.A.* **1992**, *89*, 4163−4167.
(15) Khokhlov, A. R.; Khalatur, P. G. *Physica A* **1998**, *249*, 253−261.
(16) Villeneuve, C.; Guo, H.; Zuckerman, M. J. *Macromolecules* **1997**, *30*, 3066−3074.
(17) Timoshenko, E. G.; Kuznetsov, Y. A.; Dawson, K. A. *Phys. Rev. E* **1996**, *53*, 3886−3899.
(18) Timoshenko, E. G.; Kuznetsov, Y. A.; Dawson, K. A. *Phys. Rev. E* **1996**, *54*, 4071−4086.
(19) Timoshenko, E. G.; Kuznetsov, Y. A.; Dawson, K. A. *Phys. Rev. E* **1998**, *57*, 6801−6814.
(20) Halperin, A. *Macromolecules* **1991**, *24*, 1418−1419.
(21) Ganazolli, F.; Kuznetsov, Y. A.; Timoshenko, E. G. *Macromol. Theory Simul.* **2001**, *10*, 325−338.
(22) Vasilevskaya, V.; Klochkov, A. A.; Khalatur, P. G.; ten Brinke, G. *Macromol. Theory Simul.* **2001**, *10*, 389−394.
(23) Ganazolli, F. *J. Chem. Phys.* **2000**, *112*, 1547−1553.
(24) Liu, H.; Farrell, S.; Uhrich, K. *J. Controlled Release* **2000**, *68*, 167−174.
(25) Doi, M.; Edwards, S. F. *The Theory of Polymer Dynamics*; Oxford Science: New York, 1986.
(26) Liang, H.; Chen, H. *J. Chem. Phys.* **2000**, *113*, 4469−4471.
(27) Taylor, M. P. *J. Chem. Phys.* **2001**, *114*, 6472−6484.
(28) Wu, C.; Zhou, S. *Phys. Rev. Lett.* **1996**, *77*, 3053−3055.
(29) Ganazolli, F. *J. Chem. Phys.* **1998**, *108*, 9924−9932.
(30) Sevick, E. M.; Monson, P. A.; Ottino, J. M. *J. Chem. Phys.* **1988**, *88*, 1198−1206.
(31) de Gennes, P. G. *J. Chem. Phys.* **1982**, *76*, 3316−3321.
(32) Kuznetsov, Y. A.; Timoshenko, E. G.; Dawson, K. A. *J. Chem. Phys.* **1996**, *104*, 3338−3347.
(33) Polson, J. M.; Zuckermann, M. J. *J. Chem. Phys.* **2000**, *113*, 1283−1293.
(34) Chang, R.; Yethiraj, A. *J. Chem. Phys.* **2001**, *114*, 7688−7699.


MA020741F